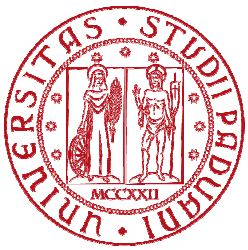

UNIVERSITA' DEGLI STUDI DI PADOVA

Dipartimento Territorio e Sistemi Agro-Forestali
Landscape, Environment, Agronomy and Forestry Department

MASTER THESIS IN

FOREST AND ENVIRONMENTAL SCIENCES

FOREST ROAD AND STAND STRUCTURE PARAMETER EXTRACTION USING LOW DENSITY LIDAR DATA

Supervisor:

Dott. Emanuele Lingua

Supporting supervisor:

Dott. Stefano Grigolato

Student:

Niccolò Marchi

Enrollment N°: 619518 AB

Academic Year 2011-12

Счастье-это быть с природой,видеть ее,говорить с ней

Лев Толстой - казаки

Happiness is being with nature, seeing her, and conversing with her

Lev Tolstoj – The Cossacks.

Contents

Abstract

Many are the modern solutions for forest planning and management. Among these, LiDAR is the one that actually catalyzes lots of the energies of forest researchers all over the world. Very versatile in most of the fields of study, is recently starting to attract even the working sector, looking for methods able to guarantee cheap, reliable and continuous data on wide scales.

The present work reports a study connected to the extraction of stands and forest roads parameters, using a low density (~1 point/m^2; 1x1 m grid) Canopy Height Model available to the public administration of the Trento province (Northern Italy).

The study has been carried on in 53 sites, following an experimental sampling design that included a road stretch of 25 m, on which have been considered a circular forest structure plot per each side, with a radius equal to 12,5 m. For each feature have been considered the major descriptive parameters and consequently analyzed through univariate and multivariate statistics.

For what concerns the road network, the influence of slope steepness and conifer cover on the recognition of the road width and longitudinal gradient was tested; the results ($p < 0,05$) suggested that the definition of the former is affected by the operator accuracy, while the latter sees in the conifer percentage its main error source.

Dealing with the silvicultural aspects, instead, structural and topographical features were analyzed all together in order to identify the relationships underlying between ground survey data and LiDAR derived ones. The major responses were connected to a good reliability of the latter in case of conifer stands, finding in broadleaves stands, high stand density and (partly) high slope steepness the factors that can worsen data.

Riassunto

“Caratterizzazione di viabilità forestale e struttura forestale attraverso l'impiego di dati LiDAR a bassa densità.”

Fra i molti ritrovati tecnologici applicati al settore forestale, il LiDAR risulta essere quello che, al momento attuale, catalizza molte delle energie dei ricercatori di tutto il mondo. Molto versatile in vari rami del settore, sta recentemente acquisendo un notevole interesse all’interno dell’ambito applicativo, in cerca di metodi che possano garantire dati economici, affidabili e continui su larga scala.

Il presente lavoro riporta uno studio relativo all’estrazione di parametri che possano caratterizzare i popolamenti forestali e descrivere la viabilità forestale utilizzando Modelli Digitali delle Chiome (CHM) a bassa densità di punti (~1 punti/m^2; griglia 1x1 m) disponibili presso la pubblica amministrazione della Provincia Autonoma di Trento.

Lo studio ha preso in esame 53 siti campione, seguendo un disegno sperimentale che prevedeva un tratto stradale di 25 metri, lungo il quale è stata considerata un’area di saggio circolare per ogni lato, di raggio pari a 12,5 m. Per ogni componente sono stati considerati i principali parametri descrittivi, successivamente analizzati attraverso statistica uni- e multivariata.

Per quanto riguarda la viabilità forestale, è stata testata l’influenza della pendenza del versante e della copertura di conifere nel riconoscimento della larghezza e pendenza del tratto stradale; i risultati ($p < 0,05$) hanno suggerito una fonte di errore dovuta principalmente all’accuratezza dell’operatore per quanto riguarda il primo parametro, mentre il secondo risulta interessato maggiormente dalla copertura dovuta alle conifere.

Riferendosi agli aspetti strettamente forestali, invece, le componenti strutturali e topografiche sono state analizzate nel loro complesso per identificare le possibili relazioni implicite tra i dati campionati sul campo e tramite LiDAR. La maggioranza dei risultati hanno portato a considerare affidabili i dati relativi a popolamenti di conifere, trovando nelle latifoglie, nell’alta densità di fusti e (solo parzialmente) nell’elevata pendenza le principali fonti di errore.

1 Introduction

In the recent years a very strong change is concerning the sector connected to the environmental mapping and management. Indeed, many are the new (and renewed) solutions that are accompanying the forester in its work, trying to compete with the well-established old tools mainly to offer a higher precision on larger scales. With them, methods are changing too, adapting to all these new possibilities that are slightly evolving.

Ground surveys have always been time and energy consuming, a characteristic that is day by day less tolerated by the modern society, that asks for huge amounts of different data on wider scales. In this perspective, in the 1850s photo interpretation moved the first step in this direction, permitting to explore and understand processes that before were restricted to the eye and personal interpretation. During the first half of the 20th century photogrammetry transformed these information into quantitative data for cartographical an topographical products. But only during 1970s, with the support of the innovative GPS systems, this technique acquired a definitive importance in the creation of Digital Terrain Models. As presented in Konecny (1985) this dynamic seems built up of 50-years cycles, characterized from the invention of a new instrumentation, its common usage for 25 years plus other 25 in which shares the market with the new one of the next cycle. In the actual phase we are observing a pretty important shift, not only in the instruments but also in the technique, as discussed in Baltsavias (1999), a passage between passive to high power active sensors, from full area coverage to pointwise sampling. It's the case of RADAR and LiDAR technologies, based respectively (as acronyms say) on RAdio or Light Detection And Ranging.

Dealing with the latter one, has to be reminded that was originally thought by NASA for topographical studies, where showed its potential in the generation of Digital Terrain Models due to the laser ability of penetrating forest canopies; furthermore, experimentations of the University of Stuttgart found out that penetration rates to the ground could range from 20-40% in European coniferous stands to 70% in deciduous ones (Ackermann, 1999). This advanced technique in all its features is a rapidly growing technology and many technical improvements have evolved in relatively few years, reducing step by step the initial disadvantages.

Thanks to its wide versatility, is well known to engineers for applications like the analysis of structural integrity of buildings, to meteorologists for the analysis of the atmosphere composition (*see* Measures, 1992) as much as for the classical topographical and hydrological purposes, slowly substituting photogrammetry. Only in the last two decades the research is focusing on the various applications even in the forestry sector (Lefsky et al., 2002), and the resultant studies indicate that the obtained data can be used in wide-scale forestry activities such as stand characterization (Naesset, 2002; Zimble et al., 2003; Maltamo et al., 2005; Sherril et al., 2008), forest inventory and management (Moskal et al., 2009), fire behaviour modelling (Mutlu et al., 2008), and forest operations (Akay et al., 2009). In the case of Italy, the usage of LiDAR data is being considered a good solution for continuing the historical series of dendrometrical data of the management plans, even in those small local administrations that cannot afford the costs of ground surveys (Abramo et al., 2007).

In this perspective, the purpose of this work is to evaluate, through the LiDAR dataset available to the public administration of the Trento Province (Northern Italy), of a forest road network and the structure dynamics of the nearby stands inside the forests of the Val di Sella valley.

1.1 LiDAR: a quick overview

A laser scanner is based on the usage of a laser (Light Amplification by Stimulated Emission of Radiation) beam to calculate the distance between the sensor and a target through the intensity and delay of the returning part of it. This creates the so called “point cloud” from which is possible to define a surface based on the different returns, and with a higher number of analyzed points per square metre the accuracy of the survey can increase till errors of few millimetres (Bienert et al., 2006).

Traditionally, even if the instrument doesn’t change so much, these devices are distinguished depending on the support on which they’re mounted:

- Terrestrial Laser Scanner (TLS): a high accuracy instrument capable of giving back a 3D image of the stand; thus, finds many applications in standing timber measurements and optimal harvest decision-making (Keane, 2007);
- Airborne Laser Scanner (ALS): usually thought for fixed-wing aircrafts, is possible to be used also on helicopters;
- Spaceborne Laser Scanner: takes often the name from the project/satellite in charge, like the well-known ICESat. For the development of this issue see Lefsky et al. (2005) and Simard et al. (2008).

For what concerns dynamic surveys (vehicles, aircrafts or satellites) the system itself is composed by a laser scanner, a position and orientation system (POS), realised by an integrated differential GPS (DGPS) and an inertial measurement unit (IMU), and the control unit (Wehr and Lohr, 1999). As all the laser systems, it measures the distance between the sensor and the illuminated spot, retrieving three-dimensional information by transmitting short-duration pulses and recording the reflected echoes, everyone of which is identified by the three spatial coordinates (x, y, z) (Gobakken and Naesset, 2009) and the so called GPS time that univocally characterize a pulse (Gatziolis and Andersen, 2008).

The very powerful laser beam used is highly directional and due to its physical characteristics has the advantage to be shot within small intervals and collimated with high precision.

On an average the wavelength available is between 800 and 1000 nm, but in this range is still capable of hurting the eye; working on higher wavelengths (near 1500 nm) is possible to reduce this inconvenient, adding also the advantage that the maximum flight range can be extended to more than 1500 m and the background sunlight radiation is very low (Wehr and Lohr, 1999). By the way it’s important to evaluate the one in use due to the fact that an extremely high can’t work properly on high reflectivity surfaces like ice.

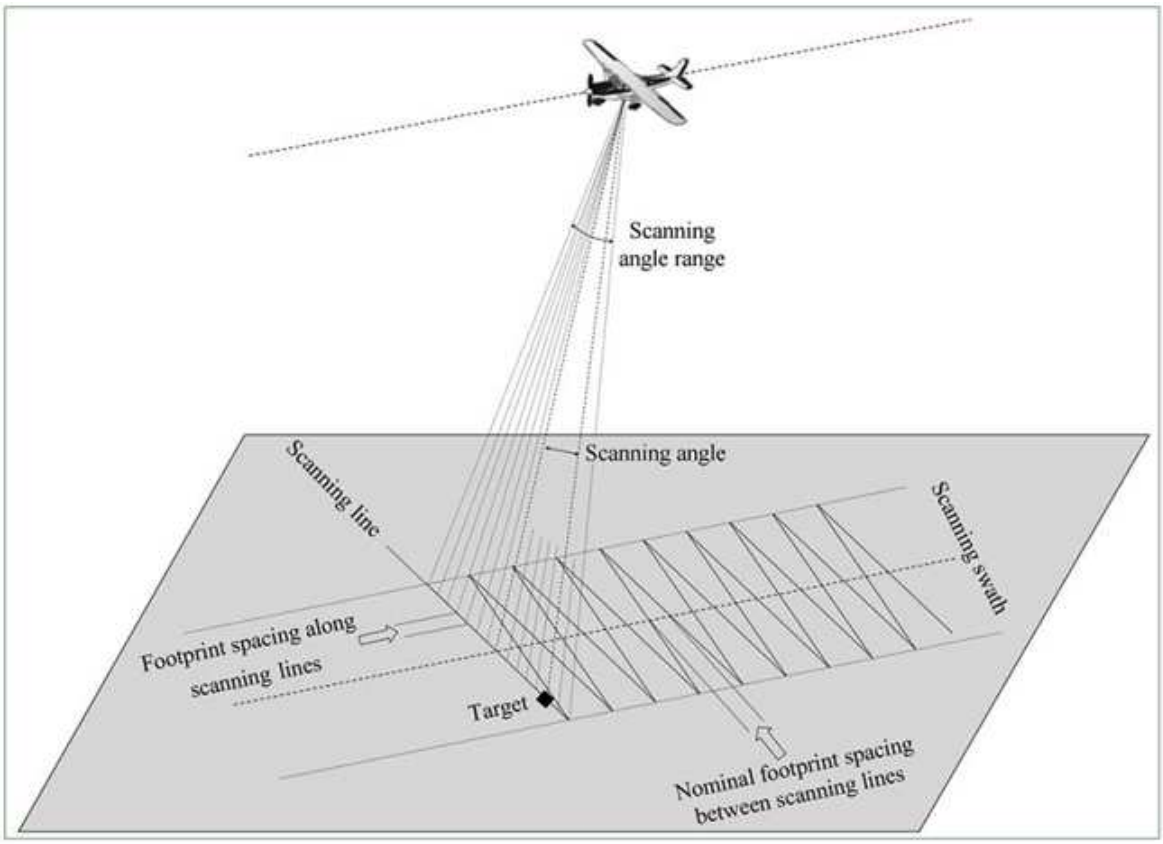

Figure 1: General scheme of an ALS survey and basic terminology (from Gatziolis and Andersen, 2008).

Here after are presented some basics about LiDAR data characteristics, following the framework given in Gatziolis and Andersen (2008):

- Scanning frequency: the number of pulses or beams emitted by the instrument in one second and, thus, defined in Hertz (Hz). With the increasing in frequency is possible to achieve higher densities of discrete returns even increasing the speed and elevation of the aircraft, accelerating the survey and reducing the relative costs;
- Scanning pattern: the spatial arrangement of the pulse returns on the target surface; can vary from seesaw to linear or elliptical, depending on the mechanism used to direct pulses across the flight line (oscillating or rotating mirror);
- Beam divergence: the beam tends not to keep the cylindrical shape of the true laser and creates a narrow cone. This divergence is measured in millirad (mrad, usually between 0,1 and 1,0) and, spreading the energy on a bigger area, brings to a lower signal-to-noise ratio

- Scanning swath: the width of the scanned path, given by the combination of the scanning angle and the aboveground flight height,
- Footprint diameter: is the diameter of the beam on the ground from a specific height; the energy is not uniform over its extent and decreases radially from the centre following a two-dimensional Gaussian distribution;
- Number of returns per beam: is the maximum number of individual returns that can be extracted from a single beam;
- Pulse density: measures the spatial resolution and depends on the ratio 1/(footprint spacing)^2, where the denominator is the distance between the centres of two beams' footprints on the same scanning line;
- Return density: often confused with the pulse density, is the mean number of returns per square metre.

2 Materials and methods

2.1 Location and main description of the study area

The study has been carried out in the Val di Sella area, a valley included in the municipality of Borgo Valsugana, in the Autonomous Trento Province (PAT). The area belongs to a single land registry but the management of forests has been officially split with the municipality of Castelnuovo because of a law dated 1871, done to solve a controversy about the usage; private property is mainly concentrated in the valley bottom and becomes public on both slopes increasing with height.

Located with an East-West disposition on the eastern side of the province, can be considered a relatively small valley (approximately 60 km^2) on the orographical right side of the Valsugana valley, that connects Trentino to the Veneto Region following the Brenta river. The main hydrography is quite limited due to the limestone substratum that drives to karstic phenomena; on the other hand, along the slopes cases of debris flow can occur where heavy precipitation encounters fragile geological structures.

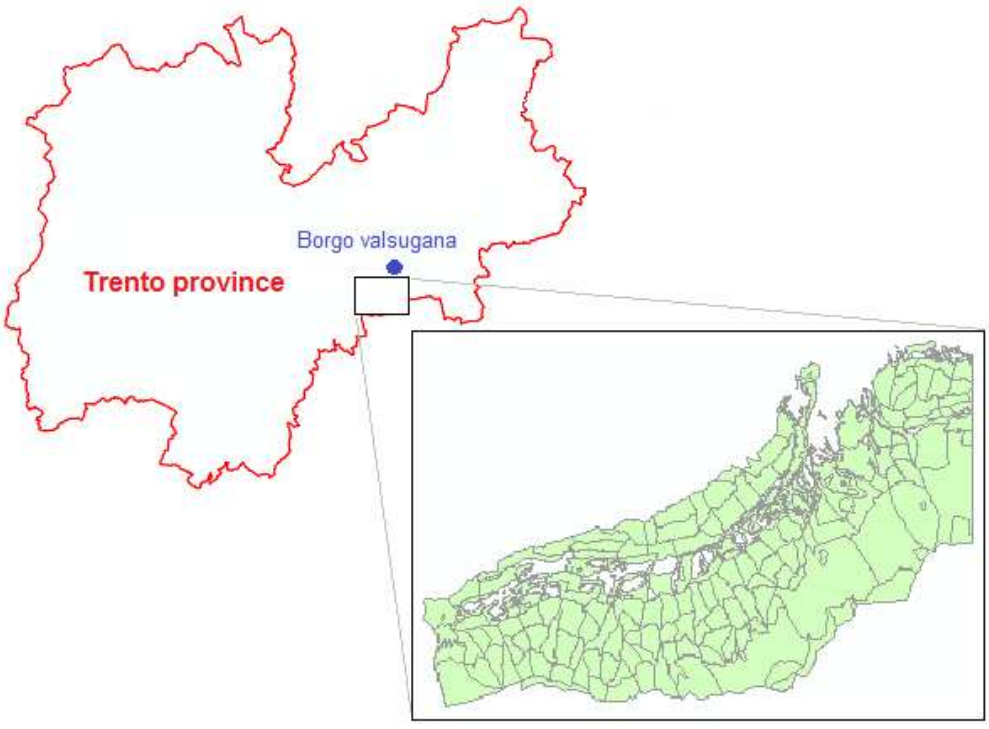

Figure 2: Overview of the study area (Val di Sella, Trento - Northern Italy).

Geology

Almost all the territory has a sedimentary geological substratum mainly Mesozoic with a moraine cover of different depth; it's also possible to find some examples of crystalline basement of Bellerophon, paleocenic marlstone and vulcanites. The limestone strata have been disconnected by some faults parallel to the Valsugana valley and running along the Sella valley bottom, Civerone and Canaia mounts. This brought to a clear differentiation of the two slopes: the right one presents all the series between the crystalline basement, the phyllites and the grey limestone, while on the other one, due to a vertical inclination given by the fault, shows more or less only the grey limestone.

Soils evolved along the limestone series, from leached brown to calcareous brown to rendzin. Many have been the factors limiting the evolution of these, due mainly to the high inclination of the slopes or insufficient vegetation cover caused by excessive cuts in the past.

Climate

The area is included in the prealpine-subcoastal climate that characterizes all the southern part of the province. The average temperature of the valley bottom is around 8° C and precipitation reaches 1100 mm per year, with peaks during spring and autumn and a summer monthly average of 100 mm. On a phytoclimatic basis can be distinguish the North slope as mesalpic from the South one that is considerable esalpic.

Vegetation

Among the factors affecting the natural vegetation dynamics, has to be mentioned the recent impact of the human activity; indeed, after centuries of light management since 3000 years ago, these areas have been destructed and overexploited during the last world conflicts. Actually, thanks to respectful management and due to the particular conformation of the valley itself, it's possible to notice a great variety of forest types in a pretty small area.

On the north slopes there's a prevalence of silver fir (*Abies alba* Mill.) stands, mixed mainly with spruce (*Picea abies* Karst.) in case of mesic conditions and with beech (*Fagus sylvatica* L.) where soil is less thick. Going upward, above 1500m a.s.l. larch

(*Larix decidua* Mill.) prevail on the previous ones and mountain pine (*Pinus mugo* Turra) covers scree.

On the other side of the valley, beech stands (partially mixed with spruce or some mesic broadleaves) dominate the slope, and these can alternate with mixed stands of Manna ash (*Fraxinus ornus* L.) and hop hornbeam (*Ostrya carpinifolia* Scop.) or Scots pine (*Pinus sylvestris* L.) stands on the Armentera mount. Finally, are present small situations like *Tilia-Acer* stands on mount Canaia and sessile oak (*Quercus petraea* (Mattuschka) Liebl.) or chestnut (*Castanea sativa* Mill.) groups on mount Zaccon.

2.1.1 Forest management

The whole territory is divided into eight land management classes organized as:

- A Class: Fir and spruce stands;
- B Class: Pine stands;
- C Class: Beech and broadleaves coppices;
- D Class: Beech high forest stands;
- H Class: Protective larch and pine stands;
- K Class: Protective broadleaves stands;
- Pastures and other crops;
- Unproductive areas

A brief *excursus* of the previous management plans is needed to understand the recent evolution of the forests of the valley in the last decades.

After the big problems connected to damages and overexploitation occurred during the World War II, appears in the management plan of 1960 the necessity for a complete change towards a new silviculture, because "*where clearcuts have been applied is still visible how the fertility of soils is decreased by the heavy leaching*".

For these reasons, (beech) coppices were driven to specific requirements:

- the selection system with target diameter equal to 8-12 cm and rotation period of 12-15 years;
- release of 2-300 standards per hectare;
- increase in the natural conifer percentage (larch and Scot pine);

- cutting of less important broadleaves.

while for high forest stands, become evenaged with the antecedent clearcuts on wide extents:

- selective felling (focused on small and medium diameters);
- respect to beech where scarcely represented.

A last concern was addressed to the poor road network.

The plan of 1970 confirmed all the above mentioned measures, fixing as a goal the increase of spruce presence, the conversion of beech coppices to high forest system and the seeding of fir on prepared sites.

The plan of 1985 added the directives about thinning of beech conversion coppices reaching the following parameters:

- unevenaged structure with mixture of species;
- growing stock values around 340 m^3/ha for Class A and 225 m^3/ha for pine stands.

The plan of 1995 focused more on high forests:

- mixed and unevenaged stands with natural regeneration of conifers and broadleaves;
- selection cut for single trees or small groups
- thinning of beech transition stands and conversion of remnant coppices;

With the actual plan these main points are carried on through a continue screening of the stands evolution; among the important features like the increase of stand diversity and productivity, is good to notice how the forest road network has reached approximately 34 linear metres per hectare, in comparison with the provincial average of 27 m/ha and the optimal one between 20 and 35 m/ha (Cielo et al., 2003). The distribution of the road system isn't properly balanced on both slopes due to the different productivity, showing a prevalence on the North one in which are concentrated the conifer high stands.

2.2 Experimental survey design

The study has been carried out considering a number of 53 areas called Compound Survey Unit (CSU), concentrated mainly in three regions inside the valley; ten have been chosen along road stretches without or with scarce tree coverage, instead of the other ones that show differences in the cover grade. Each CSU has been thought in order to analyze silvicultural and road parameters, and for this reason is made up of:

- Road survey (SU-R): identification of the centreline of a 25 metres stretch (circa) with recognition of the width, inclination, canopy coverage and its mean height;
- Sample plot area on the uphill slope (SU-U): circular, with a 12,5 m radius (~500 m^2);
- Sample plot area on the downhill slope (SU-D): circular, with a 12,5 m radius.

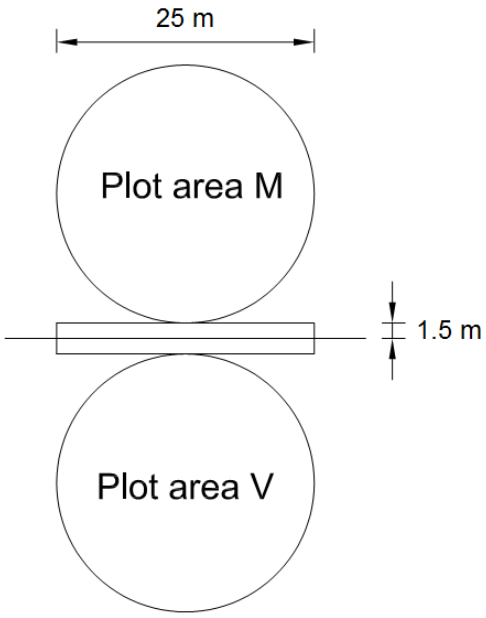

Figure 3: General layout of a Compound Survey Unit.

Three moments clearly different have characterized the study: a preliminary overview, the field survey and the data analysis. Each of them will be treated separately due to the specific purposes.

2.3 Preliminary overview

The Digital Terrain Model provided by the PAT has been used on a GIS support (ESRI ArcMap® 10) to create the *hillshade* (135° and 315°) of the area, in order to have a close-to-real image of the terrain surface. This particular feature, together with the real forest road network, has allowed the recognition of roads themselves, out of every other natural (streambeds, dales, etc) or artificial element (war artefacts, mule tracks, etc) that can disturb this process.

Afterwards, the CSU have been positioned along all the network in a random way, having care to divide them into the three regions before mentioned with a minimal distance of 150 m between each other.

The centre points have been stored into the GPS and used during the field campaign for the recognition of the possible study area. Some of them have been necessarily moved not far away because of extreme situations not previously detected by the means of the GIS maps.

2.4 Field survey

The field campaign has required about 10 days and a quite rich amount of tools was needed for all the different measurements; among the newest and very precise ones is good to mention:

- Trupulse® 360/b: a multitasking laser range finder that permits to measure slope distance, inclination, azimuth and calculate horizontal and vertical distance (www.lasertech.com);
- Pathfinder® ProXH™ GPS receiver: delivers subfoot (< 30 cm) precision (www.trimble.com); has been connected to a Trimble® "Nomad" as datalogger.

To these have been took on some of the classical instruments such as:

- Tree calliper;
- Compass: more reliable than the electronic one included into the Trupulse®;
- Metal measuring tape: for a higher precision in small measures (road width);

- GRS Densitometer™ (Figure 4): combines horizontal and vertical vegetation sampling thereby enabling the collection of resource information across the landscape (horizontally) at different canopy levels (vertically) (www.grsgis.com).

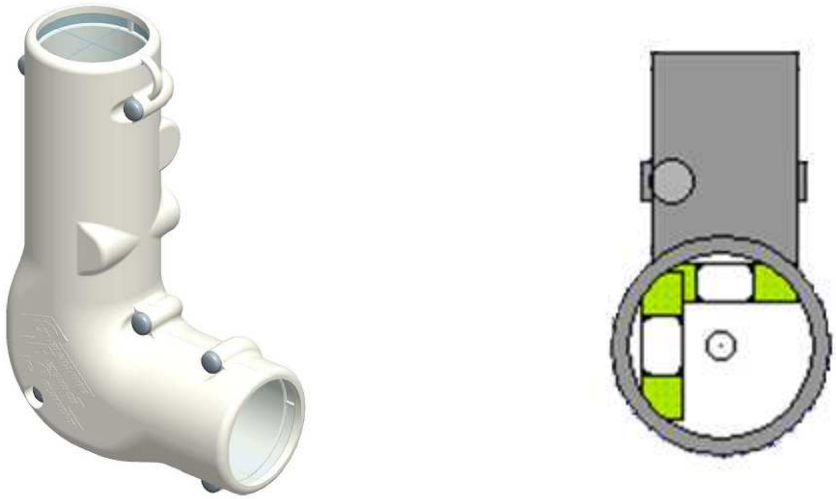

Figure 4: Vertical densitometer (on the left) and view (on the right; www.forestrytools.com).

2.4.1 Road survey

The procedure provides for the recognition of the preselected point and the settling of the GPS along the centreline, launching then the data collection. This has been set two metres high and organized for the registration of only one kind of feature (point) with a text attribute containing a progressive number for the identification of the CSU. For an ease of use and due to a satellite coverage not always optimal, in each area have been collected an amount of about 2000 signals, with low accuracy (high values of PDOP to increase production).

The length of the road stretch has been measured through the usage of Trupulse using a distance of 12,5 m for each side, keeping the GPS as reference. Along the segment has been considered the canopy coverage through a collection of full/empty records with the vertical densitometer, distinguishing the former ones depending on the kind of plant (conifer/broadleaf), useful for understanding how LiDAR data work under different leaves condition.

To complete the description of the road have also been taken in consideration:

- surface type and maintenance status;
- steepness;

- width, differentiating the carriageway from the roadbed;
- presence of water drainage structures (ditches, cross drain culverts and open-top culverts) or walls and their maintenance status;
- height of the canopies covering the centreline, divided into two classes (more or less than 12 m, considered as half of the general mean height).

2.4.2 Stand structure

For what concerns the silvicultural aspects, the centre of each plot has been identified with the same technique used for the endings of the road stretch, but with a distance of 14 metres, found as the sum of the buffer (1,5 metres) and the 12,5 metres of the plot radius. Connected to this, also the relative azimuth has been pointed out, to permit the drawing on GIS support in a later moment.

The size and shape of the sample plots have been thought due to optimize the consequent data matching and elaboration: the radius can be considered proportioned to the small diameters encountered (< 75 cm; *see* Gray, 2003) and good enough to limit the problems connected to the co-registration error and edge effect. The former depends on the overlapping grade between the ground plot and the canopy one; the latter, instead, associated with LiDAR metrics, is largely unavoidable, and related to the fact that trees located into (or out of) the plot may have part of the crown excluded (or included). For this reason has been considered the experience described in Frazer et al. (2011) in which a dataset of simulated canopies and synthetic LiDAR point clouds is processed to evaluate the effect of co-registration error on the accuracy of estimation of biomass within the variation in size of the plots. An increase in accuracy has been drawn enlarging the area from 314 m^2 (radius = 10 m) to 1964 m^2 (radius = 25 m), that changed tendency continuing to 2500 m^2; in theory, this leads to obtain less precise and accurate LiDAR metrics in sample plots with a large perimeter-to-area ratio.

The calliper threshold has been considered 7,5 cm and for each tree has been considered also the specie and the height class; this has been obtained dividing by four the mean value of the 3-4 highest individuals per plot, in order to have the possibility to draw a rough standard height curve.

To complete the site description have been noted the slope gradient and every kind of useful information like terrain roughness, natural regeneration, recent stumps, etc.

2.4.3 LiDAR data

Data have been collected through two different sensors in a time span of about two years, from October 2006 and February 2008, during a mapping campaign that covered the whole Province. The products were a Digital Terrain Model and a Canopy Height Model, both with a grid made of cells 1 x 1 m.

All the relative characteristics are reported below in the Table 1.

Table 1: Specifications of the flights that collected the dataset used (www.territorio.provincia.tn.it).

Sensor	OPTECH ALTM 3100C	TOPOSYS II
Aircraft	PARTENAVIA P68 (Fixed wing)	CASA 212C (Fixed wing)
Altitude	1000-1800 m (a.g.l.?)	1500 m (a.g.l.?)
Mean speed	250 Km/h	350 Km/h
Pulse rate	100 KHz	85 KHz
Sampling density	1,28 p/m^2	0,48 p/m^2
Mean distance between points	0,9 m	1,5 m
Wavelength	0,4-0,8 nm	1,56 nm
Scan angle	25°	7°
Planimetric precision	1/2000 of relative flight altitude $1\sigma \equiv \pm 1$ mt $\div 2\ \sigma$ 1/3000 of relative flight altitude $2\sigma \equiv \pm 1$ mt $\div 2\ \sigma$	
Altimetric precision	15-30 cm 1 σ	
Echoes	2 (first and last)	
Period	October-December 2006, 2007, January-February 2008	

The PAT states that with such a planimetric precision, the detail can be compared to a cartography on a scale 1:5000, and the DTM is comparable to the ones made by a photogrammetric stereo compilation (Cekada, 2009). Indeed, for the same scale, recently

has been proposed on an empirical base an optimal point density of about 12-20 points per square metre (Cekada, 2010).

All GPS and LiDAR data are based on the UTM-WGS84 coordinate system, considered as a default setting in the PAT.

2.5 Data elaboration and analysis

Collected data have been stored into different databases dividing road features from stand structure ones, in order to facilitate the following steps.

First, GPS points have been corrected with data coming from the close permanent station situated in the town of Spera, around 10 kilometres away. Even if the initial accuracy wasn't extremely high, the differential correction brought almost the 70% of measurements to be in an error range between 0 and 50 centimetres. Through the GPS management software Trimble® PathFinder Office® a shapefile has been exported with the centres of the single CSUs and later was imported into ESRI ArcGis.

For each single point has been manually traced a segment of about 25 metres along the carriageway, for which have been extracted the extremes (*Data Management/ Features/Feature Vertices to Points* using the function *Both Ends*) and calculated the altitude values from the DTM (*Extract Values to Points*), which have been later used for the estimation of the road steepness. Furthermore, the width has been measured on GIS environment

The canopy cover has been considered on a CHM filtered in order to exclude heights below two meters as in White et. al. (2010), which has been intersected with the road segments (*Zonal statistics as table*); the same operation has been done with the DTM to calculate the vegetation cover as the proportion between CHM cells on the total amount of matching ones.

The tool *Bearing distance to line* has permitted to obtain the centres of the stand sample plots, from which have been calculated the altitude values for the calculations concerning the mean slope gradient. Furthermore, a buffer equal to 12,5 metres has been created around these points in order to draw the circular area of each plot. This feature, kept separated between SU-D and SU-U, has been used as a mask for the counting per rank of

the CHM cells included (Z*onal histogram*) and the calculation of the relative heterogeneity indexes.

The variables taken in consideration are:

- CSU slope steepness (SlopeSt): measured on the field;
- Arithmetical mean diameter (Dmean);
- Arithmetical mean diameter standard deviation (D_STD);
- Quadratic mean diameter (Dmean_BA);
- Stand density (per hectare):
    - Stems (stems/ha): for a consideration valid for all stand types;
    - "Stumps" (stumps/ha): for comparison of the unit per area distribution between high forest stands and coppices;
- Basal area (per hectare; G/ha);
- Indexes:
    - Tree Height Diversity (THD) index (Kuuluvainen et al., 1996): applied to the four tree height classes recognized during the field work;

$$THD = -\sum_{i=1}^{n} p_i \, log_e p_i$$

where p_i is the proportion of individuals (trees) in the i^{th} height class and n is the number of diameter classes;

    - Tree Diameter Diversity (TDD) index (Rouvinen and Kuuluvainen, 2005): applied to 10 cm diameter classes;

$$TDD = -\sum_{i=1}^{n} p_i \, log_e p_i$$

where p_i is the proportion of individuals (trees) in the diameter class i, and n is the number of diameter classes;

    - Gini coefficient (Gini, 1912): a measure of heterogeneity that quantifies the deviation from perfect equality and has a minimum value of zero,

when all categories are of equal size; applied to the diameters, to the canopy cover and to the CHM cells.

$$G = 1 - \sum_{i=1}^{n} p_i^2$$

where p_i is the proportion of individuals (trees) in the i th height class and n is the number of diameter classes;

- Zonal statistics: descriptive variables based on the GIS analysis of the CHM cells:
  - COUNT: the amount of cells included into the defined area;
  - AREA: calculated on the base of the cell size;
  - MINIMUM: the smallest value of all cells included into the defined area;
  - MAXIMUM: the largest value of all cells included into the defined area;
  - RANGE: the difference between the largest and smallest value of all cells included into the defined area;
  - MEAN: the average of all cells included into the defined area;
  - STD: the standard deviation of all cells included into the defined area;
  - SUM: the total value of all cells included into the defined area;
  - VARIETY: the number of unique values for all cells included into the defined area;
  - MAJORITY: determines the value that occurs most often of all cells included into the defined area;
  - MINORITY: determines the value that occurs least often of all cells included into the defined area;
  - MEDIAN: determines the median value of all included into the defined area;
- Maximum height
  - (field survey): stand height based on the largest height value of the three highest trees;
  - (LiDAR-derived): stand height based on the cell with the highest value;
- Mean height:
  - (field survey) obtained considering the average of the height of the three tallest individuals;

    - (LiDAR-derived) calculated from the CHM (>2 metres) considering the average of the three cells with the highest value;
- Weighted mean height: based on the closest multiple of four to the mean height, the frequency of individuals included in each of the four height classes individuated during the ground survey have been multiplied by the mid-class value.
- Conifers' basal area: the amount of conifer basal area;
- Broadleaves' basal area: the amount of broadleaf basal area.

For a pre-check of the correlation among variables, a matrix containing all data has been analyzed considering the Spearman correlation coefficient for four different cutoff values (0 – 0,25 – 0,5 – 0,75) with *p*-values equal to 0,05 , 0,01 and 0,001.

Then has been applied a screening of the dataset to prepare it for the statistical analysis, basing the choices mainly on:

a. deleting sites with no significance (e.g.: an area that was set in a meadow);
b. deleting all the records that contained missing values in some of the variables.

Lately, data have been organized creating a main matrix with the LiDAR-derived variables and a secondary matrix with those obtained from the field sampling; each variable has been standardized on its STD (*Modify data → Relativization → Adjust on standard deviate*).

A cluster analysis (*Groups → Two way cluster analysis*) has been used to check which variables were more self-correlated, in order to simplify the matrices from redundant data. Referring to the obtained dendrograms (Figure XX and XX) has been possible to individuate some grouped variables that, cross-checked with the previously elaborated correlations, have been selected as follows:

1. LiDAR-derived variables (Figure 5). Excluded:
    a. RANGE, MAX and Hmax_G in favour of Hmean_G;
    b. SUM and MEDIAN because less significant than MEAN;
    c. MAJORITY and MINORITY because of their lack of meaning for a stand description;

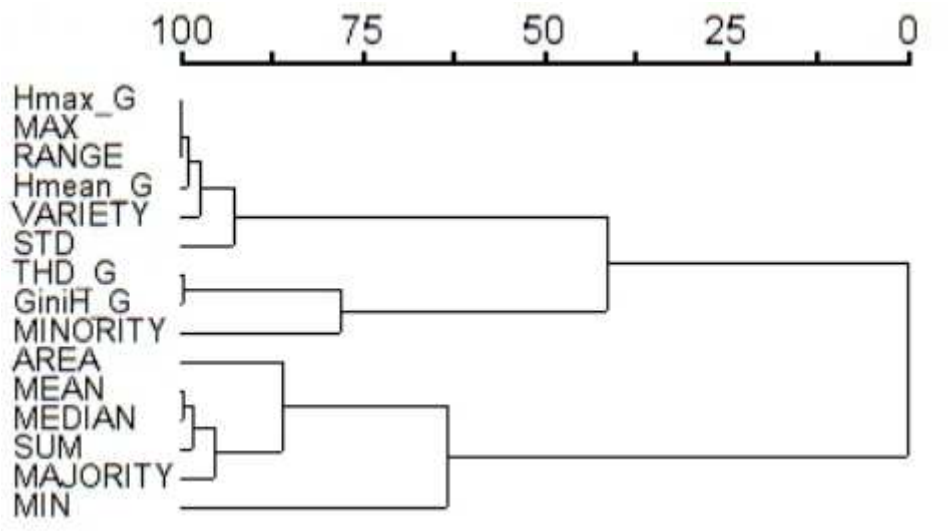

Figure 5: Dendrogram of LiDAR-derived variables.

2. field-derived parameters (Figure 6). Excluded:
    a. stumps density in favour of stem density;
    b. Dmean and G/ha in favour of Dmean_BA;
    c. Hmax in favour of Hmean.

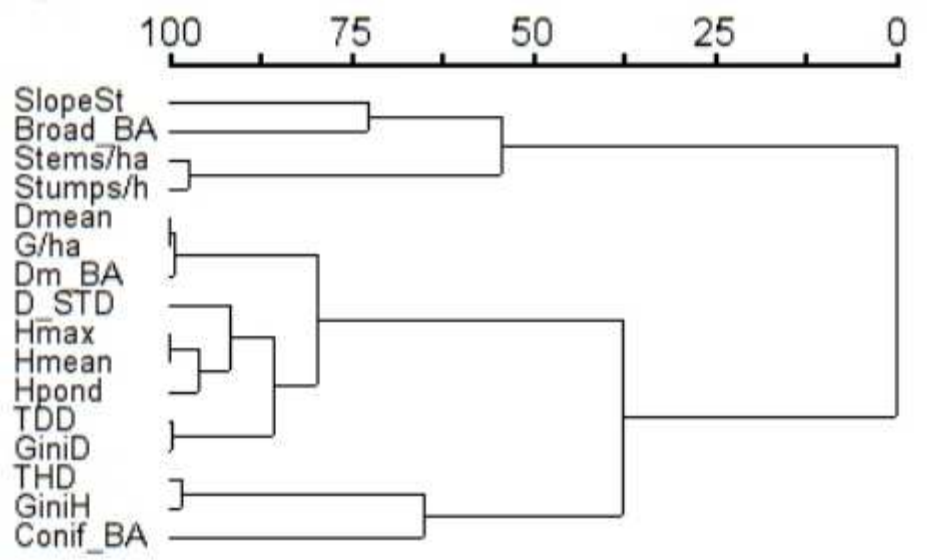

Figure 6: Dendrogram of the field parameters.

Variables using the Gini index were preferred to THD and TDD.

An outlier analysis (*Summary* → *Outlier analysis* ; Figure 7) has been carried on to individuate the presence of more sites with low significance; these were filtered setting a threshold equal to two times the STD.

```
****************************** Outlier Analysis ******************************
PC-ORD, 6.0
 2 Feb 2012, 15:47:03

outlier


    Frequency distribution of average distances    N =    92 SmplUnit

 Distance*   |  Frequency   (each "X" represents one entity)
-------------|-------------------------------------------------------------------------
     9.29830 |X 025V
     8.83394 |
     8.36957 |
     7.90521 |
     7.44084 |
     6.97648 |
     6.51211 |
     6.04775 |XX 027V     041M
     5.58338 |XX
     5.11902 |XXXX
     4.65465 |XXXXX
     4.19029 |XXXXXX
     3.72592 |XXXXXXXXXXXXXXXX
     3.26155 |XXXXXXXXXXXXXXXXXXXXXXXXXXXXXXX
     2.79719 |XXXXXXXXXXXXXXXXXXXXXXXXXXX
-------------------------------------------------------------------------------------------
* Distances at left are lower end of that bin`s range.
```

Figure 7: Results from the outlier analysis, showing the sites with low significance.

Finally, a redundancy analysis (*Ordination* → *RDA*) has been run on the obtained matrices, in order to check for the underlying relationships. The analysis settings provided for centred but not standardized responses, scaling for correlation biplot and graphing based on linear combinations of fitted site scores (explanatory variables).

3 Results

3.1 Road analysis

A first descriptive overview of the available data (Table 2) gave a rough idea of the mean characteristics of the road network of the valley.

Tabella 2: General descriptive features of the road network surveyed.

Road surface				Drainage					
Type		Maintenance		Type				Maintenance	
G	N	R	S	A	Ot	Cd	D	R	S
53	0	50	3	29	22	1	1	13	11

G: gravel, N: natural, R regular, S: scarce, A: absent, Ot: open-top culvert, Cd: cross drain culvert, D: ditch

The surface for the primary forest road system provides for the gravelling in a good maintenance condition; indeed, only the 3% of the SCUs were present with a scarce condition, connected to the fact that were in a road stretch isolated by a landslide some years before.

The main road geometry is the outsloped type that, connected to the medium road mean steepness (around 8,7%), explains why the drainage system covers on an average the 45% of the network; the most used water management turned out to be the open-top culvert, present within the 92% of the cases, with single presences of a cross-drain culvert and a natural ditch. For what concerns the maintenance, it was already applied in the 46% of the situations, but workers teams were starting the regular cleaning during the field campaign period (first half of October).

The following statistical analysis of the road parameters has been carried on using the software StatGraphics® Centurion.

Data have been organized on a table containing values of maximum width (Wmax, measured from the toe of cut to the top of fill slopes, soft shoulders included), real width (Lut, meant as carriageway), road steepness (P), mean slope steepness (Pm_v, considered as original shape before road construction, calculated as average of values detected for the single sample plot on each road side) and vegetation cover (Conif). The latter has been

considered only as conifer percentage due to its importance as a disturb factor during LiDAR winter flights.

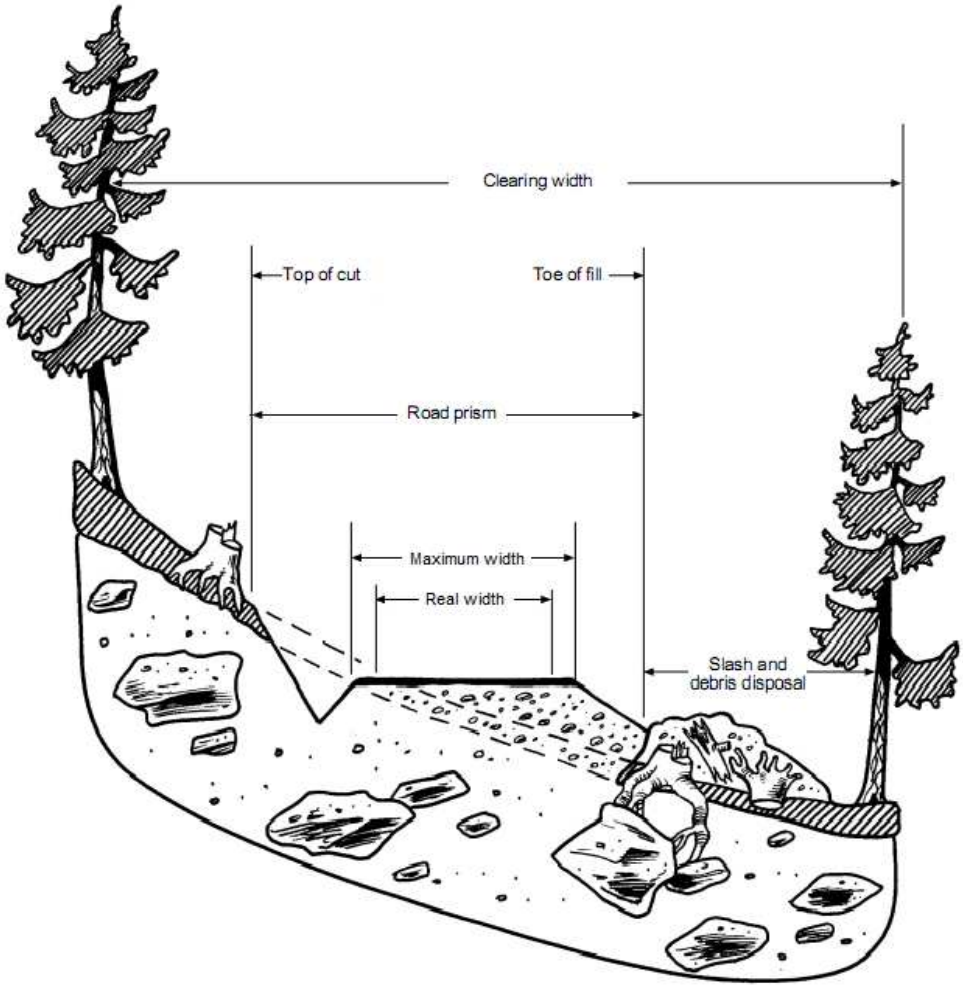

Figure 8: Basic nomenclature of road features (BCMF, 2002; modified).

Some parameters have been reclassified, for a matter of ease during the ANOVA test, with the first letters of the alphabet; the road slope has been divided into two classes with 10% breaks (A = 0-10%, B = 10-20%), conifer percentage (Conif) and mean slope steepness (Pm_v) in four classes with 25% breaks.

For a quick overview, the above mentioned parameters can be summarized briefly as in Table 2, Table 3 and Table 4 (suffix G marks GIS measured data):

Table 3: Summary table for mean width values.

Description	*Value*	*Unit*
Real	3	m
Max	3,5	m
Max_G	3,3	m
Error	18,4	%
RMSE	0,82	m

Table 4: Summary table for mean slope values.

Description	*Value*	*Unit*	*A (0-10)*	*B (10-20)*	*Unit*
Avg	8,7	%	52,8	47,2	%
Avg_G	8,2	%	58,5	41,5	%
Error	17,6	%			
RMSE	2,06	%			

Table 5: Summary table for factors characteristics (Conif – conifer cover , Pm_v – mean steepness of the slope).

	A (0-25)	*B (25-50)*	*C (50-75)*	*D (75-100)*	*Unit*
Conif	75,5	13,2	5,7	5,7	%
Pm_v	11,3	26,4	41,5	20,8	%

Two analysis procedures have been applied on these parameters:

a. a comparison of the samples (field and GIS), to assure the relative independency of data; this was carried on through
    - a “t-test”: to verify the equality of the means;
    - a “test F”: to compare the standard deviations;
    - a “Kolmogorov-Smirnov test”: to compare the distributions;
b. the “ANOVA” test to identify factors affecting the relative errors.

3.1.1 Maximum width

The comparison between the field data ad GIS ones has shown that differences are statistically significant, as it’s possible to see below in the Table 6:

Table 6: Summary table for statistics on width values.

	Unit	*Wmax*	*Wmax_G*
Count	N°	53	53
Mean	m	3,51887	3,34528
Standard deviation	m	0,574475	0,776225
Coeff. of variation	%	16,3256	23,2036
Minimum	m	2,3	2,0
Maximum	m	5,8	5,9
Range	m	3,5	3,9
Std. skewness	-	**3,815**	**2,661**
Std. Kurtosis	-	**6,178**	1,96487

Values of standardized skewness and kurtosis exceed the range between -2 and +2, showing a relevant shift from normal distributions. Further tests like comparison of means or standard deviations could not be valid due to this situation.

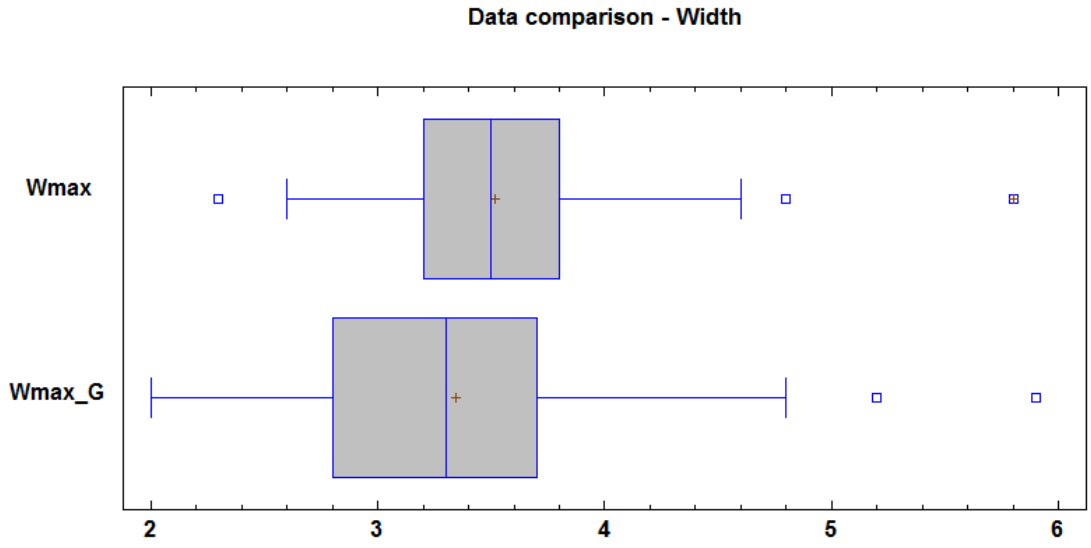

Figure 9: Comparison between field (Wmax) and GIS (Wmax_G) maximum width.

3.1.2 Slope

For what concerns the two measurement groups on steepness, no statistical differences have been noticed.

Table 7: Summary table of statistics on slope values.

	Unit	*P*	*P_G*
Count	N°	53	53
Mean	%	8,7	8,17
Standard deviation	%	4,2	4,471
Coeff. of variation	%	47,9	54,728
Minimum	%	1,1	0,2
Maximum	%	16,5	16,8
Range	%	15,4	16,6
Std. skewness	-	-0,731892	0,014
Std. Kurtosis	-	-1,4458	-1,570

As visible in the table above, both values of standardized skewness and kurtosis are included into the expected range, meaning that the samples follow a normal distribution. This is also confirmed by the variances analysis and the Kolmogorov-Smirnov test, both with a confidence interval equal to 95%.

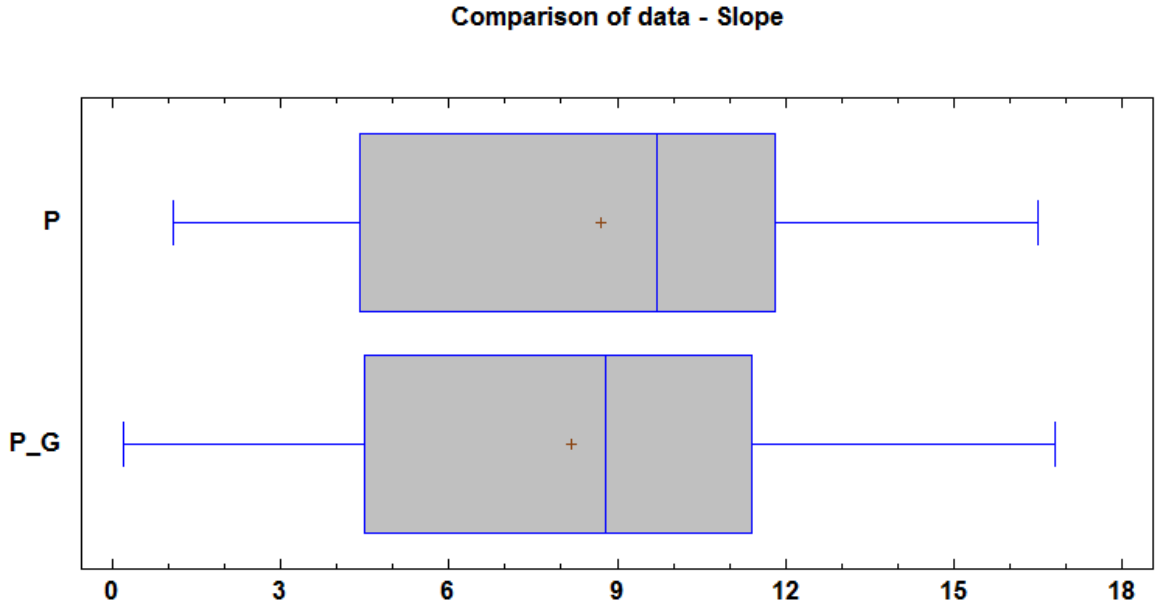

Figure 10: Comparison between field (P) and GIS (P_G) slope data.

3.1.3 Error factors

The ANOVA analysis has been carried on considering factors like conifer cover and mean slope steepness as interference in GIS measurements, both classified as previously written (suffix "CL" stands for "classes").

The width error (W_err) couldn't have been considered into the test due to the lack of statistical meaning already explained in 4.1.1; that's why will be listed only the calculation reports on the slope error (P_err) analysis.

Table 8: Variance analysis for P_err – Sum of squares, Type III.

Source	*Sum of squares*	*Deg. f.*	*Mean of squares*	*F Ratio*	*P-value*
MAIN EFFECTS					
A:Conif_CL	5722,27	3	1907,42	5,49	**0,0026**
B:Pmv_CL	1836,84	3	612,278	1,76	0,1678
RESIDUE	15989,7	46	347,601		
TOTAL (CORRECT)	23401,1	52			

Table 9: Least squared means of P_err, with confidence interval equal to 95%.

Level	*Count*	*Mean*	*Standard Error*	*Lower Limit*	*Upper Limit*
MEAN	53	24,1176			
Conif_CL					
A	40	14,9853	3,24704	8,44929	21,5212
B	7	13,0007	7,75429	-2,60792	28,6093
C	3	7,65852	10,8971	-14,2763	29,5934
D	3	60,8259	11,1856	38,3105	83,3414
Pmv_CL					
A	6	13,9467	8,0146	-2,1859	30,0793
B	14	24,8642	5,9711	12,8449	36,8834
C	22	22,6664	5,62175	11,3504	33,9824
D	11	34,9932	7,13193	20,6373	49,349

Being statistically significant as a "disturb factor", the four classes of conifer cover have been singularly described (Table 10) and then compared in pairs (Table 11).

Table 10: Multiple range test using LSD method with confidence interval equal to 95%.

Conif_CL	*Count*	*Mean of L. squared*	*Sigma of L. squared*	*Homogeneous groups*
C	3	7,6585	10,897	X
B	7	13,001	7,754	X
A	40	14,985	3,247	X
D	3	60,826	11,186	X

Table 11: Multiple range test using LSD method with confidence interval equal to 95%.

Contrast	*Sig.*	*Difference*	*+/- Limits*
A - B		1,985	16,030
A - C		7,327	22,97
A - D	*	**-45,841**	23,677
B - C		5,342	27,221
B - D	*	**-47,825**	28,501
C - D	*	**-53,167**	30,984

* marks a statistically significant difference.

3.2 Stands

The correlation analysis didn't permit to apply a first-glance selection of data, due to the pretty high values of Spearman coefficients that weren't limited by the *p*-value but were subjected to a significant reduction in matching relationships only with a cutoff equal to 0,500.

The screening procedure presented in Paragraph 2.5 permitted to reduce the considered data, respectively from 106 to 89 for the plots and from 31 to 16 for the variables; in spite of this, the dataset could have been thought robust enough for all the above mentioned statistics.

The usage of the RDA highlighted the consideration of only three of the six possible Axes, explaining through the first two a variance equal to 60,3 % (Figure 11).

```
VARIATION IN MAIN MATRIX REPRESENTED BY SECOND MATRIX
             6 = number of canonical axes
    3.72279    = sum of all canonical eigenvalues
    6.00000    = total variance in response variables (main matrix)
       0.620465 = proportion of variance in main matrix explained by predictors


AXIS SUMMARY STATISTICS
Number of canonical axes: 3 of     6 possible.
Total variance in the species data:     6.000
-----------------------------------------------------------
                                  Axis 1   Axis 2   Axis 3
-----------------------------------------------------------
Eigenvalue                         3.098    0.521    0.065
Variance in species data
     % of variance explained        51.6      8.7      1.1
     Cumulative % explained         51.6     60.3     61.4
Pearson Corr., Response-Pred.*     0.929    0.549    0.453
Kendall Corr., Response-Pred.      0.739    0.342    0.303
-----------------------------------------------------------
* Correlation between sample scores for an axis derived from the response
     variables (main matrix) and the sample scores that are linear combinations
     of the predictors (second matrix).
     Set to 0.000 if axis is not canonical.
```

Figura 11: Axis summary statistics report.

Plotted LiDAR-derived data (Figure 12) have shown a negative correlation in the first Axis, with high rates for variables connected to mean values (Hmean_G and MEAN) and heterogeneity (VARIETY and STD). The second Axis is described more by variables such as GiniH_G, AREA and MEAN; the former expresses a positive relationship, suggesting an increase in heterogeneity of the cells with the increase of the Axis.

On the other hand, the second matrix (based on the field data) shows an Axis 1 characterized again by strong negative correlations except for the stem density (stems/ha) and in a minor way for Broad_BA and SlopeSt; Axis 2, instead, has its strongest relations with GiniH (positive), Hpond and again with stem/ha (negative).

FINAL SCORES for 6 ExplVars

		Axis 1	Axis 2	Axis 3
1	Hmean_G	-0.288532	-0.045252	1.112163
2	GiniH_G	-0.139262	0.684601	-2.137894
3	AREA	-0.073853	-0.888436	-2.609144
4	MEAN	-0.246779	-0.697155	1.182996
5	STD	-0.266131	0.364650	0.600345
6	VARIETY	-0.288098	0.202465	-0.979471

CORRELATIONS AND BIPLOT SCORES for 10 ExplVars

		Correlations*			Biplot Scores		
	Variable	Axis 1	Axis 2	Axis 3	Axis 1	Axis 2	Axis 3
1	Slope_St	0.236	-0.233	0.062	0.236	-0.233	0.062
2	D_STD	-0.732	0.175	-0.092	-0.732	0.175	-0.092
3	Dm_BA	-0.803	-0.192	0.285	-0.803	-0.192	0.285
4	Stems/ha	0.609	-0.318	-0.403	0.609	-0.318	-0.403
5	GiniH	-0.328	0.384	-0.595	-0.328	0.384	-0.595
6	GiniD	-0.666	-0.242	-0.274	-0.666	-0.242	-0.274
7	Hmean	-0.984	-0.065	-0.037	-0.984	-0.065	-0.037
8	Hpond	-0.875	-0.320	0.149	-0.875	-0.320	0.149
9	Conif_BA	-0.712	-0.041	-0.324	-0.712	-0.041	-0.324
10	Broad_BA	0.337	0.073	0.161	0.337	0.073	0.161

* Correlations are "intra-set correlations", i.e. between fitted site scores and predictors.

Figure 12: Final scores and correlation tables of the two matrices.

Almost all the variables considered have been graphically represented through proportional vectors in a dispersion graph based on the two most significant axes; the R squared cutoff was set to 0,100 not to exclude the slope steepness, even if all the remaining variables had values bigger than 0,500 .

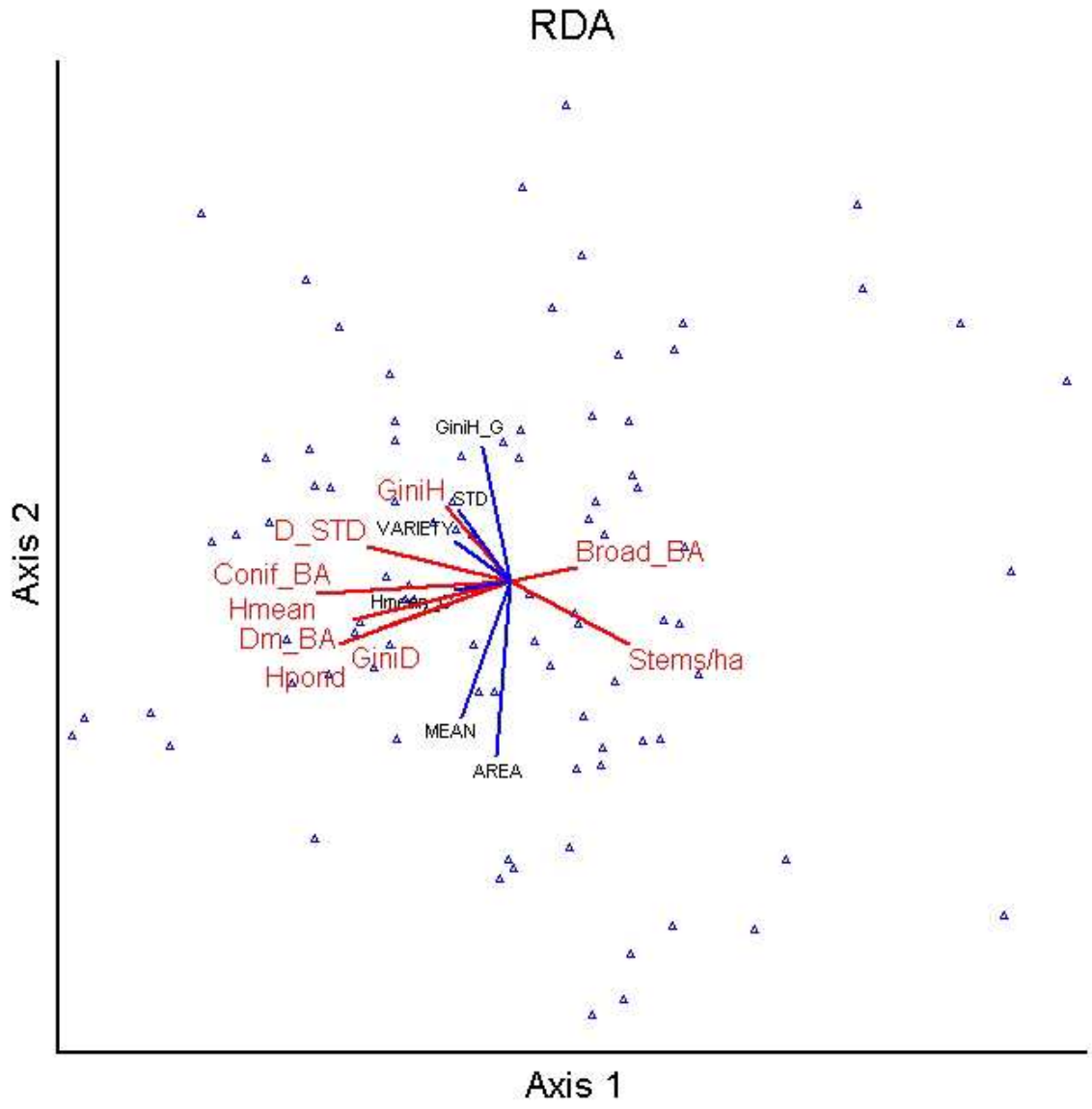

Figura 13: Redundancy analysis (RDA) graph; blue vectors for the variables of the main matrix (LiDAR-derived data) and red for the ones of the second (field survey).

The software permits to modify the obtained graph by rotating it by 30° in a clockwise direction (Figure 14), making the slope steepness vector appear; this can happen due to a change in the reference axes during the rotation, with a consequent worsening of data in favour of a slightly clearer representation.

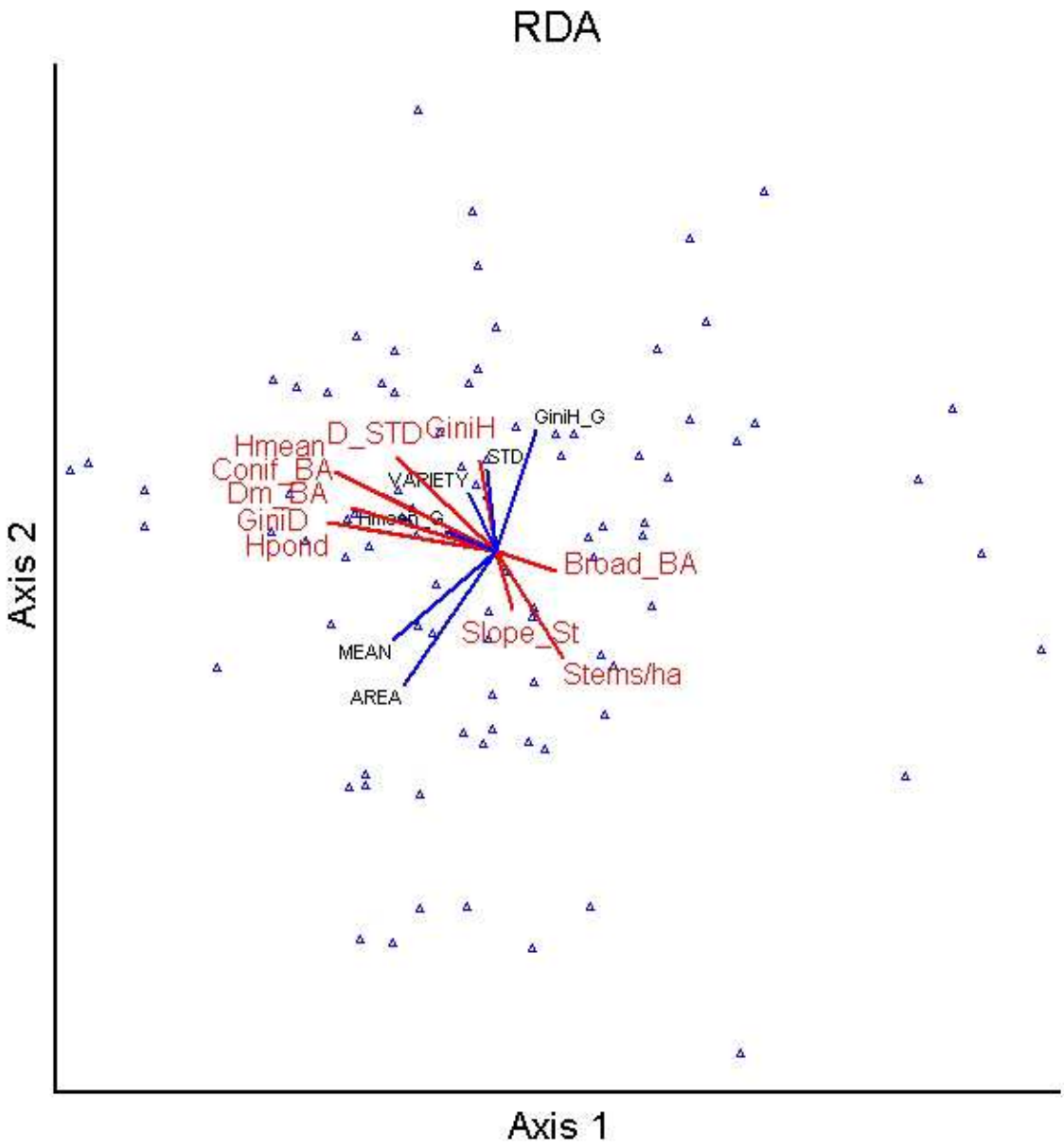

Figure 14: RDA graph rotated by 30° in a clockwise direction.

3.3 LiDAR data quality

A problem arose because, on the GIS support, some points were not precisely located in the middle of the carriageway as measured in the field; indeed, some of them were slightly shifted towards the roadside, while others were completely out of the track (positioning error ranging from 0,4 to 4 metres from the expected real point). Initially has been thought that this could be connected either to a misleading of the *hillshade* or to an instrumental error in the data collection, but afterwards seemed clear that were not.

Figure 15 represents an overview of a sample road taken for LiDAR quality evaluation; the stretch length is equal to about 600 metres, in which are situated five CSUs studied during the same field-work day.

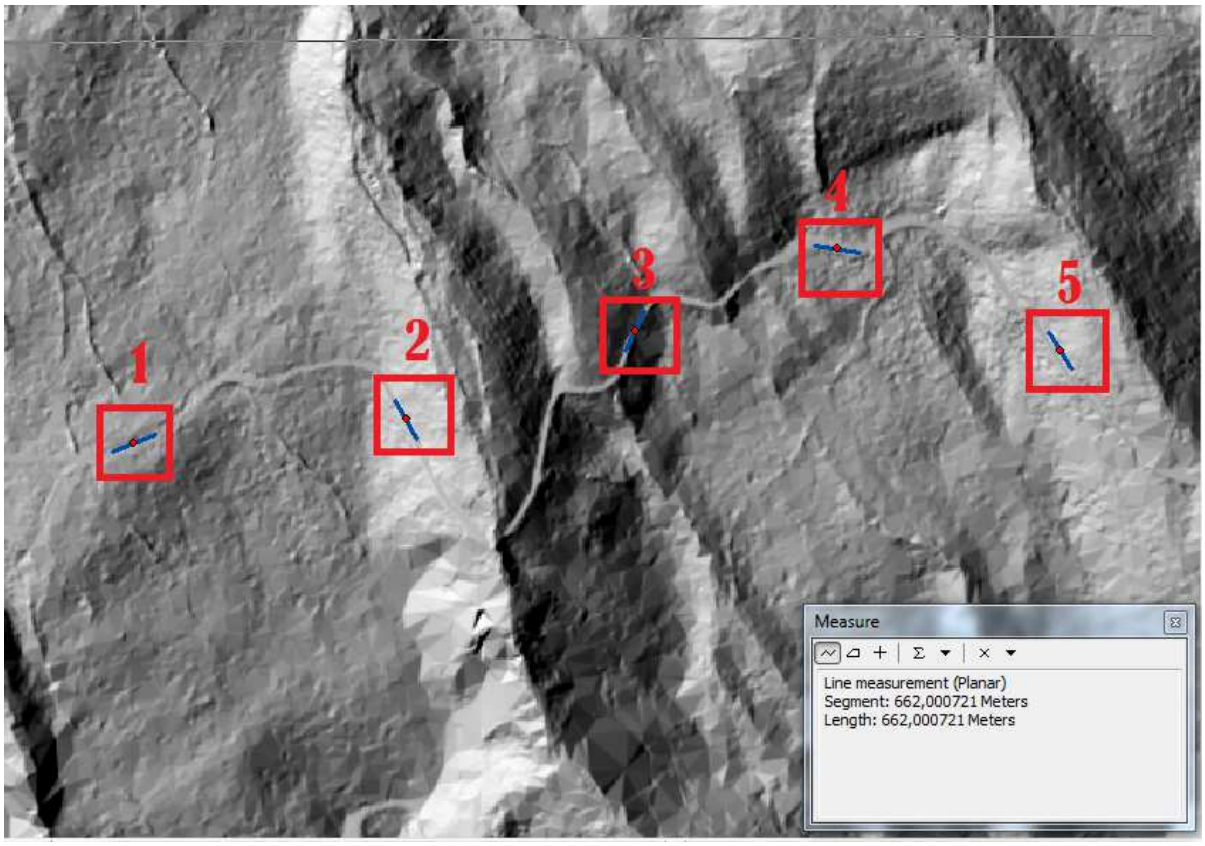

Figure 15: Overview of the sample road stretch for LiDAR quality evaluation (scale 1:3000).

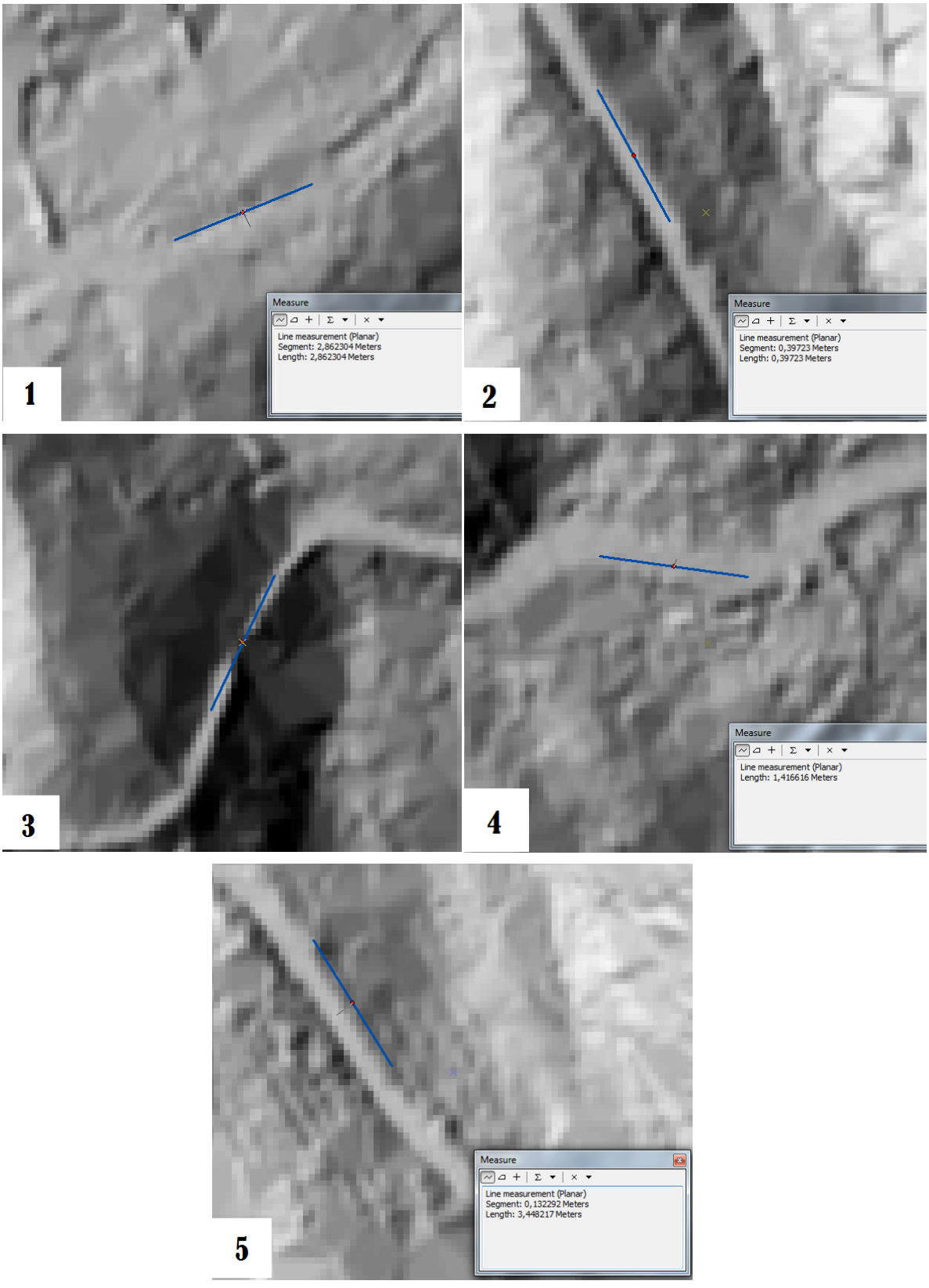

Figure 16: Detail of the single sample areas (scale 1:500).

1. Road non easily recognizable; medium positioning error (2,9 m);
2. Well defined road; very small positioning error (0,4 m)
3. High vegetation cover lowers the road definition; no references for the error estimation.
4. Pretty well defined road; small positioning error (1,4 m).
5. Well defined road; big positioning error (3,4 m).

On a overall glance of the valley has been possible to identify a slight tendency in the location error of the points. Indeed, the ones with an error higher than one metre (that could be thought as limit, being the sum of mean LiDAR and GPS data) is shifted towards the valley bottom. A possible explanation could be connected to the dependence of point location to the flight direction. Unfortunately hasn't been possible to deepen the issue because too energy requiring and not to get out of topic.

Even if such situation was valid for a big number of points of the total amount, calculations continued keeping these "error points" following the purpose of the study: to estimate the suitability of using these datasets commonly available to public administration of the PAT.

3.4 Costs and benefits considerations

Some considerations have to be done for the evaluation of the costs connected to the acquisition, processing and use of such datasets. Data available on the web is not sufficient for a complete overview of the issue, because of the scarcity, the unbalanced provenience and the lack of recent sources; hence will be presented only a brief glance. For a matter of ease costs are reported with time-discounted Euro values and measures expressed according to the International System.

For what concerns the United States of America, it's possible to see a modified scheme proposed by Renslow et al. (2000) reported in Table 12; it's based on mobilization, reference station survey, aircraft costs, IMU & ABGPS services, LIDAR with 3-4 meter post-spacing, and pre and post-processing for a bare earth DEM and SEM formatted for GIS.

Table 12: Costs for LiDAR per area range (Renslow, 2000; modified).

Extent range (ha)	*Cost per hectare (€)*
2000 - 4000	9,0
4000 - 12000	7,5
16000 - 24000	7,0
24000 - 40500	6,0
40500 - 101000	5,0
> 101000	4,5

Hallum and Parent (2008) report cases like Minnesota, where is reached a cost/benefit ratio equal to 3,5 (per each dollar spent 3,5 are saved) or the one of Nebraska where state-wide efforts range from 26 to 39 € per squared kilometre ($83 to $122 per square mile); no time reference is given to understand these values.

In Hummel et al. (2011) is suggested an average cost of acquisition and processing ranging between 1,5 and 2,5 €/ha on areas from 36.000 to 12.000 hectares (2 and 3 dollars respectively on areas from 90.000 and 30.000 acres).

Related to Europe, and specifically to Italy, Barilotti (2010) describes an average of 4-6 €/ha for a hypothetical helicopter scanning of 10.000 ha, with point density equal to 5 pts/m^2 and the point cloud as main product.

Finally, in Australia, Turner (2007) registers a pretty wide costs spectrum depending on the quality required and kind of survey, ranging from 0,5 to 10 € per hectare.

4 Discussion

Important!

Unfortunately, is necessary to highlight a problem connected to the scarce availability of data dealing with all the possible vegetation cover situations, realized only during the analysis phase; the study indeed was thought as a collection of data useful for both the purposes initially proposed and, in order to consider them statistically correct, the sample plots have been taken randomly in the whole valley.

4.1 Road survey

Tests conducted on the available data have confirmed some simple concepts that was necessary to control. Results on maximum width (W_max) listed in 3.1.1. show clearly how a relationship is missing between the two samples compared; this can surely be referred to the fact that width parameters manually measured on the screen are affected by the grid accuracy and operator skilfulness. In addition, the ANOVA test contributed affirming that the GIS measurements (and hence in its error, W_err) aren't influenced by the mean slope steepness (Pm_v) or conifer cover (Conif).

In an operational situation the noticed differences would not be a real problem, due to the fact that the GIS support would be used as a reference to control the network characteristics needed in the moment; for real road design new methodologies are being elaborated from some professionals (Dalle Donne, 2011) that require more precise LiDAR data such as grids 0,5x0,5 m.

For what concerns the stretch steepness (P) and its error (P_err), things are pretty different. The two samples considered for the analysis of the former come from the measure of an unbiased feature, limiting the biggest errors to the instrumental ones; this brought, indeed, to identify them as part of normal distributions. On the other hand, it's interesting to see how the conifer percentage in the vegetation cover affects the reliability of P_err data; indeed Table 11, dealing with the multiple range test, shows a relevant discrepancy between the group with values below 75% (classes A, B, C) versus the one (D) above this level: it's a good signal to interpret such measurements as no more trustworthy.

4.2 Stands

The big amount of results reported in the previous Chapter are a source of abundant information, that need to be considered in singular steps.

At a first glance, a comparison of results with the correlation table confirms the steps followed, specifically in relation with the exclusion of many LiDAR-derived variables (MAX, RANGE, MIN, MEDIAN, SUM), obtained from the same GIS tool due to their very high self-correlation.

Pretty similar the case about the choice between indexes (THD, TDD Vs Gini) correlated per typology with values above 0,95 and $p < 0,001$.

Many are also the ecological relationships underlying the RDA responses, some of which are inside the same matrix and others between the two.

For what concerns the first matrix, appears clear the inverse relation between AREA and cells variability (GiniH_G and STD), that can represent the possibility in which a higher ground cover decreases the heterogeneity of the vegetation height, independently to the value of the latter (Hmean_G).

Moreover, the second matrix shows different interesting aspects. One case is the inverse relation between Stems/ha and structure diversity (D_STD and GiniH), very representative for young and dense stands where stratification and diameters' diversification are not still active due to the high potential that the most of individuals have. Another case is the one related to the decrease in Dm_BA following an increase in Broad_BA, probably due to the different management amontg the various stands (high forest Vs coppice) and to the bigger target diameter applied in the conifer stands in comparison to the broadleaves' one.

A pretty expected correlation for LiDAR data is the one between the increase of Broad_BA followed by a progressive underestimation of Hmean_G, while instead is possible to see a general decrease in the Hmean of stands.

An unexpected implication consists in the strong relationship ($r = 0,783$; $p < 0,001$) between Hmean and Hmean_G; indeed, even if the procedure is the same for both the variables, there is a difference in the origin data (top heights Vs CHM cells). Thinking to the kind of flight collected data (winter) this can be explained with the high

percentage of conifer stands or simply conifers that, even if scarcely present, tend to characterize the highest individuals inside the stand.

On a wider perspective, this concept allows to consider the distribution of the variables on the graph space. The main concentration on the left side of structural parameters, among which Conif_BA plays a particular role, may suggest the suitability of winter flights in determining such variables with a good significance.

On the opposite side, instead, are located those variables that are not reliable or can be source for possible errors, as the broadleaf's basal area (Broad_BA), the stem density (Stems/ha) and, in a minor part, the slope steepness (SlopeSt). In the Val di Sella valley these three factors can be found mainly in the South slope where, increasing with altitude, there is a passage from the mixed stands of the valley bottom to the broadleaves high forest stands and finally to broadleaves coppices on steep terrain.

About this spatial distribution of vectors, a note is necessary, because the very high explanatory percentage of the first Axis could influence strongly also the statistical elaboration of the few variables on the opposite direction, forcing a not so real parameter concentration.

Finally, it's necessary to remind and consider that the field campaign period can contribute a not negligible bias, because data have been collected approximately 4-5 years later compared to the LiDAR flight, in a valley were wood harvesting is still pretty active.

5 Conclusions

Many are the studies related to LiDAR data application in the forestry sector, exploring all the various aspects that can simplify and improve the work of the professionals.

The possibility of a direct comparison in the usage of the same LiDAR dataset for two different purposes has granted a valuable occasion to test its feasibility in a hypothetical planning situation. Such an aim requires to acquire information about stands characteristics and all the necessary to organize at best the harvesting operations reducing, as much as possible, the loss in time connected to field surveys. Moreover, the availability of low density data, has allowed to create a sort of close-to-real simulation, at least for what may concern the Italian situation.

The results obtained have offered a clear idea of the usage of such data in cases close to the alpine environment. In the detail, has been possible to see how the conifer presence can be considered in two opposite ways depending on the specific goal: an interference for the estimation of road characteristics (in particular the stretch steepness) and a reference point for stand parameters extraction. At the same time, regarding the latter, have been found good relations among variables, with an interesting connection ($r = 0,783$; $p < 0,001$) in the calculation of mean height between LiDAR and field data through the three tallest individuals/highest cells. Being also all the other parameters pretty well correlated, has to be considered that such results work properly if applied to conifer stands.

Considering an economical point of view and what presented in Paragraph 3.4, is possible to agree with Turner (2007) regarding LiDAR as a more accurate and cost-effective alternative to conventional photogrammetry particularly in dense forests where the ground is not visible; in addition, for what concerns areas with limited accessibility, double-sampling with LiDAR becomes cost effective for coefficient of determination 0.7 or greater as LiDAR plot costs fall below 35% of ground plot costs (Tilley et al., 2005).

In conclusion, data presented give support to the usage of low density LiDAR datasets for common forest planning with the related advantages connected to ease of use, rapidity and economical saving; furthermore, this finds a common base with the authors

listed in Grigolato (2009), dealing with the minimum requirements for specific aims as recognition of forest roads, cable crane tracing or classification of served forest areas.

Acknowledgements

Some kind of job somewhere is waiting so, ending this work, it's necessary to thank who permitted me to arrive here:

First of all, the Forest and Wildlife Office [IT: Ufficio Foreste e Fauna] of the Trento province, especially in the person of Dott. Wolynski, Dott. Olivari and Geom. Dalle Donne with all the personnel of the District of Borgo Valsugana for the helpfulness and hospitality.

All my friends, in and out of Italy to have put up with me in every single moment (and they well know how difficult it is!). It's dreadful not to thank each one singularly, but I'm so lucky to have too many that accompanied my steps since long ago, teaching me with a word or an act what friendship really is. A special word is necessary for the colleagues M.S. without which my illness for botany wouldn't have bloomed, A.S. that has been a mentor even outside the forest, A.C. which taught me perseverance through a smile, F.C. for being the best sparring partner in all the worst situations and G.P. for having helped me out with the field campaign work (just for fun).

And last, but not the least, my family for having supported me with lots of patience in all the "strange" things I did (and they still don't understand completely), especially my mother and the trustworthy washing machine.

References

ABRAMO E., BARILOTTI A., SEPIC F., 2007. Dalla dendrometria diametrica alla dendrometria ipsometrica: stima del volume degli alberi da rilievi laser-scanning, Forest@ 4 (4): 373-385.

ACKERMANN F., 1999. Airborne laser scanning: present status and future expectations, ISPRS Journal of Photogrametry & Remote Sensing 54, pp. 64-67.

AKAY A.E., OGUZ H.,KARAS I.R., ARUGA K., 2009. Using LiDAR technology in forestry activities, Environmental Monitoring Assessment (2009) 151: 117-125.

BALTSAVIAS E.P., 1999. A comparison between photogrammetry and laser scanning, ISPRS Journal of Photogrammetry & Remote Sensing 54, pp. 83-94.

BARILOTTI A., 2010. La tecnologia LiDAR nel settore forestale, in Ciclo di Seminari "Nuove tecnologie per i tecnici forestali", Firenze 15-16 Novembre 2010 e Val di Fiemme 22 Novembre 2010, ARSIA.

http://www.rivistasherwood.it/download/cat_view/169-corsi/170-corsi-arsia-cdf-novembre-2010/173-lidar.html

BCMF → British Columbia Ministry of Forest, 2002. Forest road engineering guidebook, Forest practices code of British Columbia Guidebook.

BIENERT A., SCHELLER S., KEANE E., MOHAN F., 2006. Application of terrestrial laser scanners for the determination of forest inventory parameters, in Proceedings of the ISPRS Commission, V Symposium "Image engineering and vision metrology", Dresden 25-27 September 2006, Volume 36, Part 5.

CEKADA M., CROSILLA F., FRAS M., 2009. A Simplified Analytical Model for a-priori Lidar Point-positioning Error Estimation and a Review of Lidar Error Sources, Photogrammetric Engineering & Remote Sensing No. 75, No. 12, December 2009, pp. 1425–1439.

CEKADA M., CROSILLA F., FRAS M., 2010. Theoretical LiDAR point density for topographic mapping in the largest scales, Geodetsky vestnik 54/3, 403-416.

CIELO P., GOTTERO F., MORERA A., TERZUOLO P., 2003. La viabilità agro-silvopastorale: elementi di pianificazione e progettazione, IPLA 106 pp., Torino.

Comune di Borgo Valsugana – Piano di assestamento dei beni silvo-pastorali, Validità 2006-2015, n° 357

Comune di Castelnuovo – Piano di assestamento dei beni silvo-pastorali, Validità 2006-2015, n° 347

DALLE DONNE R., 2011. Personal communication.

FRAZER GW., MAGNUSSEN S., WULDER M.A., NIEMANN K.O. 2011. Simulated impact of sample plot size and co-registration error on the accuracy and uncertainty of LiDAR-derived estimates of forest stand biomass, Remote Sensing of Environment 115 (2001) 636-649.

GATZIOLIS D., ANDERSEN H.E., 2008. A guide to LiDAR data acquisition and processing for the forests of the Pacific Northwest, General Technical Report PNW-GTR-768. Portland, OR: U.S. Department of Agriculture, Forest Service, Pacific Northwest Station, 32p.

GOBAKKEN T., NAESSET E., 2009. Assessing effects of positional errors and sample plot size on biophysical stand properties derived from airborne laser scanner data. Canadian Journal of Forest Research 39: 1036-1052.

GINI C., 1912. Variabilità e mutabilità. Bologna.

GRAY A., 2003. Monitoring stand structure in mature coastal Douglas-fir forests: effect of plot size, Forest Ecology and Management 175, 1-16.

GRIGOLATO S., 2009. Pianificazione delle utilizzazioni forestali: potenzialità dei Modelli Digitali del Terreno, Sherwood n° 156, Settembre 2009.

HALLUM D., PARENT S., 2008. Developing a business case for State-wide Light Detection And Ranging data collection: Improving Nebraska's Topographic Dataset, enhancing our quality of life, fostering engineering and scientific understanding and saving money, Nebraska Department of Natural Resources. (http://watercenter.unl.edu/PRS/PRS2009/Posters/Hallum%20Doug.pdf)

HAMMER Ø., HARPER D.A.T., RYAN P.D., 2001. PAST: Paleontological Statistics Software Package for Education and Data Analysis, Palaeontologia Electronica 4(1): 9pp. http://palaeo-electronica.org/2001_1/past/issue1_01.htm .

HUMMEL S., HUDAK A.T., UEBLER E.H., FALKOWSKI M.J., MEGOWN K.A., 2011. A Comparison of Accuracy and Cost of LiDAR versus Stand Exam Data for Landscape Management on the Malheur National Forest, Journal of Forestry – July/August 2011.

LEFSKY M.A., COHEN W.B., PARKER G.G., HARDING D.J., 2002. LiDAR remote sensing for ecosystem studies, Bioscience Vol.52 n° 1, pp. 19-30.

LEFSKY M.A., HARDING D.J., KELLER M., COHEN W.B., CARABAJAL C.C., DEL BOM ESPIRITO-SANTO F., HUNTER M.O., DE OLIVEIRA R. Jr, 2005. Estimates of forest canopy height and aboveground biomass using ICESat, Geographical Research Letters vol. 32 (2005) L22S02.

KEANE E., 2007. The potential of terrestrial laser scanning technology in pre-harvest timber measurement operations, COFORD Connects, April 2007.

KONECNY G., 1985. The International Society for Photogrammetry and Remote Sensing - 75 Years Old, or 75 Years Young, Keynote Address, Photogrammetric Engineering and Remote Sensing, 51(7), pp 919-933.

KUULUVAINEN T., PENTTINEN A., LEINONEN K., NYGREN M., 1996. Statistical opportunities for comparing structural heterogeneity in managed and primeval forests: An example from the boreal forest in southern Finland, Silva Fennica 30 (2-3): 315-328.

MALTAMO M., PACKALéN P., YU X., EERIKAINEN K., HYYPPA J., PITKANEN J., 2005. Identifying and quantifying structural characteristics of heterogeneous boreal forests using laser scanner data, Forest Ecology and Management 216, 41 – 50.

MEASURES R.M., 1992. Laser remote sensing – Fundamentals and applications, Krieger Publishing Company, Malabada (Florida).

MOSKAL L.M., ERDODY T., KATO A., RICHARDSON J., ZHENG G., BRIGGS D., 2009. LiDAR application in precision forestry, SilviLaser (2009).

MUTLU M., POPESCU S.C., ZHAO K., 2008. Sensitivity analysis of fire behaviour modelling with LiDAR-derived surface fuel maps, Forest Ecology and Management 253: 1, pp. 289-294.

NAESSET E., 2002. Predicting forest stand characteristics with airborne scanning laser using a practical two-stage procedure and field data, Remote Sensing of Environment 80 (2002) 88 – 99.

RUOVINEN S., KUULUVAINEN T., 2005. Tree diameter distributions in natural and managed old *Pinus sylvestris*-dominated forests, Forest Ecology and Management 208, 45-61.

SHERRILL K.R., LEFSKY M.A., BRADFORD J.B., RYAN M.G., 2008. Forest structure estimation and pattern exploration from discrete-return lidar in subalpine forests of the central Rockies, Canadian Journal of Forest Research 38: 2081–2096 (2008).

SIMARD M., PINTO N., FISHER J.B., BACCINI A., 2008. Mapping forest canopy height globally with spaceborne LiDAR, Journal of Geophysical Research vol. 116 (2011), G04021, 12 pp.

TILLEY B.K., MUNN I.A., EVANS D.L., PARKER R.C., ROBERTS S.D., 2005. Cost considerations of using LiDAR for timber inventory. Pages 43-50 in: Proceedings of the 2004 Annual Southern Forest Economics Workshop.

TURNER R., 2007. An overview of Airborne LIDAR applications in New South Wales state forests, ANZIF Conference - Coffs Harbour - June 2007.

WEHR A., LOHR U., 1999. Airborne laser scanning – an introduction and overview, ISPRS Journal of Photogrammetry and Remote Sensing 54 (1999) 68-82.

WHITE R.A., DIETTERICK B.C., MASTIN T., STROHMANN R., 2010. Forest road mapped using LiDAR in steep forested terrain, Remote Sensing 2, 1120-1141.

ZIMBLE D.A., EVANS D.L., CARLSON G.C., PARKER R.C., GRADO S.C., GERARD P.D., 2003. Characterizing vertical forest structure using small-

footprint airborne LiDAR, Remote Sensing of Environment 87 (2003) 171 – 182.

Software

ESRI ArcGis 10®

Trimble PathFinder Office® 4.10

StatGraphics® Centurion

PAST ™

PC-ORD®

Attatchments

1. Field sheet

GPS/SU_____ File name_____ Date_____

Geometry		Paving		Artifacts			H_canopy	
Width	Slope	Type	Maint.	Drainage (Type / Maint.)		Walls	<12m	>12m
Coverage	Full							/
	Empty							

SU-U Slope (%) _____ Azimuth _____

Specie	D	H	Specie	D	H	Specie	D	H	Heights
									Roughness.

NOTES

SU-D Slope (%) _____ Azimuth _____

Specie	D	H	Specie	D	H	Specie	D	H	Heights
									Roughness

NOTES

2. Sperman correlation summary table.